Vision Based Control Law for Agricultural Machines

D. KHADRAOUI*, C. DEBAIN**, P. MARTINET*,
M. BERDUCAT** and J. GALLICE*

* Lasmea, Université Blaise Pascal U.R.A. 1793 du CNRS,
F63177 Aubière cedex, France
** Cemagref, Domaine des Palaquins,
F03150 Montoldre, France
e-mail : Djamel.Khadraoui@lasmea.univ-bpclermont.fr

Abstract: In this paper we present a method of vision based control for agricultural machine, used to mow a vegetation. The problem we plan to resolve is the servoing task accomplishment by using visual information provided by camera, embedded on the machine. In this context, visual feedback is incorporated directly in the control loop. It deals with different aspects of the system: modelling of the scene which is represented by the limit of mowed and unmowed zone of a vegetation, modelling of the machine, and designing of a lateral controller. Experimentation results, tested on a *CEMAGREF (French Intitute of Agricultural and Environmental Engineering Research)* prototype machine, prove the feasibility of the approach and show the robustness and stability of the vision based control law.

Keywords: Vision Based Control, Real-time, Agricultural machine, Kinematic Modelling, Pole Assignment.

1. INTRODUCTION

A significant amount of research work has received considerable attention in the domain of agricultural robotics. This subject covers a wide range of potential applications, from the inspection and/or collection of fruits or vegetables to the conception of autonomous robot working in the agricultural environment. Computer vision can therefore be of significant value in order to automatically (or semi-automatically) drive a robotic apparatus which aims at replacing human beings in repetitive or hard tasks in a natural environment (Sandini 1990)(Jarvis 1990)(Derras 1993)(Amat 1993).

Today, techniques of visual servoing are used to control robot manipulators (Chaumette 1990) (Espiau 1992) (Motyl 1993) (Khadraoui january-1995) but there are still few applications in mobile robotics (Pissard-Gibollet 1991) (Jurie 1994) (Khadraoui june-1995). For a mobile robot, the main problem in using these techniques is due to the presence of non-holonomic mechanical connections which limit robot movements. In this context, traditionnal visual control laws are in general synthesized by separating the vision aspect to the control module.

In the work discussed here, we mean by visual based control aspect, incorporating visual feedback directly in the control loop of the system. Precisely, we present a method of real-time automatic control of an agricultural machine as a mobile robot used to mow a vegetation by vision. Our application involves controlling the lateral side of the machine which follows the line representing the limit between mowed and unmowed zone of vegetation, for example. The problem we plan to resolve is the servoing task accomplishment by using visual information provided only by a camera sensor, embedded on the machine. We present a general approach which gives theoretical motivation on the integration of visual information in the control closed loop. It consists of studying and applying this control loop in order to have general expression of gains of the control law.

Classical methods, which are implemented for agricultural vehicles guidance are based on vision in 3D space (Klassen 1994)(Debain april-1994). But with the visual servoing technique, the philosophy consists of reaching a particular configuration in the 2D image plane and not a situation between camera and object. So, this approach has the advantage of avoiding the intermediary step of 3D estimation of the environment with regard to the robot and then to eliminate problems related to the reconstruction of the 3D world. To use our idea we combine the different modellings of the system (camera, scene and machine). This leads us to have the behaviour of the machine in the 2D measurement image space. Therefore, we build a complete model integrating all the parts of the system in order to elaborate the control law in state space representation.

The paper is organized as follows. In Section 2, we deal with the modelling of the scene representing the limit of mowed and unmowed zone of vegetation, and the modelling of the machine which is directed by its rear wheels. In Section 3, we develop the problem of the control, elaborating the linear control law. This one depends only on the 2D visual features of the straight line considered with the (θ, ρ) parameters. In Section 4, we give the results of the control algorithm tested in different situations and realized in natural environment.

2. MODELLING

2.1 Modelling of the Scene

(Chaumette 1990)

2.1.1 **Problem Statement.** We develop the problem considering that the camera used, is modelled by the classical *pinhole* approximation and we assume that the focal length is equal to unity (see Figure 1). At each time, the 3D space point

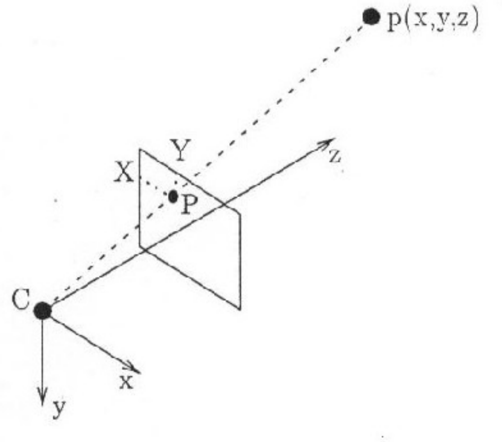

Fig. 1. Perspective Projection

$\underline{p} = (x, y, z)$ is projected onto the image plane as a point $\underline{P}$ with coordinates (X, Y) such as:

$$\begin{cases} X = x/z \\ Y = y/z \end{cases} \tag{1}$$

Knowing the camera velocity screw T_c, defined by three translational velocities $\underline{V} = (V_x, V_y, V_z)$ and three rotational one $\underline{\Omega} = (\Omega_x, \Omega_y, \Omega_z)$, this corresponds to the motion of the object in the 3D scene. These velocities can be expressed by the velocity screw T_c by means of:

$$\dot{\underline{p}} = -\underline{V} - \underline{\Omega} \wedge \underline{p} \tag{2}$$

By differentiating (1) and using (2), we can derive the well known equation relating *optical flow* measurement to 3D structure and motion in the scene. We have:

$$\begin{pmatrix} \dot{X} \\ \dot{Y} \end{pmatrix} = L_{of}\, T_c \tag{3}$$

and we obtain:

$$L_{of} = \begin{pmatrix} -1/z & 0 & X/z & XY & -(1+X^2) & Y \\ 0 & -1/z & Y/z & 1+Y^2 & -XY & -X \end{pmatrix} \tag{4}$$

This equation gives us an interaction relation between the 2D world (image plane) and the 3D one (object frame).

2.1.2 **General Method.** In general, a 3D geometrical primitive can be represented as a vectorial function like this:

$$h(x, y, z, Q_i) = 0 \tag{5}$$

This one is projected in the image frame under the following form :

$$g(X, Y, R_i) = 0 \tag{6}$$

where Q_i and R_i are the parameters of the primitives respectively in the 3D scene and in the 2D image plane. From these assumptions, we can establish the interaction screw H_i between primitive R_i and the velocity screw $T_c = (\underline{V}, \underline{\Omega})$. The set of elements H_i is grouped under the matrix $L_{\underline{s}}$ assuming that $\underline{s}$ represents the set of 2D primitives R_i. This matrix is computed assuming the following hypothesis:

$$\begin{cases} g(X, Y, R_i) = 0 \\ \dot{g}(X, Y, R_i) = 0 \end{cases} \tag{7}$$

After some developments, we obtain:

$$\sum_{i=1}^{n} \frac{\partial g}{\partial R_i} \dot{R}_i = -\frac{\partial g}{\partial X} \dot{X} - \frac{\partial g}{\partial Y} \dot{Y} \tag{8}$$

Equation (7) allows us to relate the variation of the parameters $\dot{R}_i$ to the optic flow components L_{of} and thus, to the velocity screw T_c of the camera by means of equation (4).

2.1.3 **Case of Lines.** In three-dimensionnal frame, a line is defined by two plans which intersect:

$$\left\{ \begin{array}{lcl} a_1x + b_1y + c_1z + d_1 & = & 0 \\ a_2x + b_2y + c_2z + d_2 & = & 0 \end{array} \right. \quad (9)$$

By using perspective projection, we immediately obtain :

$$\frac{1}{z} = \frac{-(a_ix + b_iy + c_iz)}{d_i} \quad (10)$$

The equation of the line in 2D space, resulting on the projection of the 3D one in the image frame (except if $d_1 = d_2 = 0$), is expressed by :

$$AX + BY + C = 0 \quad (11)$$

such us:

$$\begin{array}{lcl} A & = & (a_1d_2 - a_2d_1) \\ B & = & (b_1d_2 - b_2d_1) \\ C & = & (c_1d_2 - c_2d_1) \end{array} \quad (12)$$

We choose the (θ, ρ) parametrisation of the line which is given by :

$$g(X, Y, R) = \rho - X\cos\theta - Y\sin\theta = 0 \quad (13)$$

with :

$$\left\{ \begin{array}{l} \theta = \arctan\frac{B}{A} \\ \rho = \frac{-C}{\sqrt{A^2+B^2}} \end{array} \right. \quad (14)$$

By using (7) and (8) we calculate the differential of expression (13), we construct the interaction matrix associated to the (θ, ρ) representation of the line. We find:

$$\dot{\rho} + (X\sin\theta - Y\cos\theta)\dot{\theta} = \dot{X}\cos\theta + \dot{Y}\sin\theta \quad (15)$$

With substituting the expressions of X and $1/z$ according to Y, in the equation of *optical flow*, we find the expression of interaction matrix, by identifying term to term. We have:

$$\dot{\underline{s}} = L_{\underline{s}}^T \cdot T_c \quad (16)$$

where $L_{\underline{s}}^T$ is the interaction matrix related to the situation $\underline{s}$, expressed by :

$$L_{\underline{s}}^T = \left(\begin{array}{cccccc} \lambda_\theta\cos\theta & \lambda_\theta\sin\theta & -\lambda_\theta\rho & -\rho\cos\theta & -\rho\sin\theta & -1 \\ \lambda_\rho\cos\theta & \lambda_\rho\sin\theta & -\lambda_\rho\rho & (1+\rho^2)\sin\theta & -(1+\rho^2)\cos\theta & 0 \end{array} \right) \quad (17)$$

with

$$\left\{ \begin{array}{lcl} \lambda_\theta & = & (a_i\sin\theta - b_i\cos\theta)/d_i \\ \lambda_\rho & = & (a_i\rho\cos\theta + b_i\rho\sin\theta + c_i)/d_i \end{array} \right.$$

The scene is represented by a straight line for which we find an equation in the image frame of the camera. We express the position of the machine and its orientation according to the (θ, ρ) parameters of the line, measured in the image.

2.2 Modelling of the Machine

For the machine (see Figure 2), we establish the general equations relative to its behaviour taking into account its kinematic characteristics. It is useful to approximate the kinematics of the steering mechanism by assuming that the two rear wheels turn slightly differentially. Then, the instantaneous center of rotation can be determined purely by kinematic means. This amounts to assume that the steering mechanism is the same as a bicycle. Let the angular velocity vector directed along y axis be called $\dot{\psi}$ and the linear one directed along x axis called $\dot{x}$.

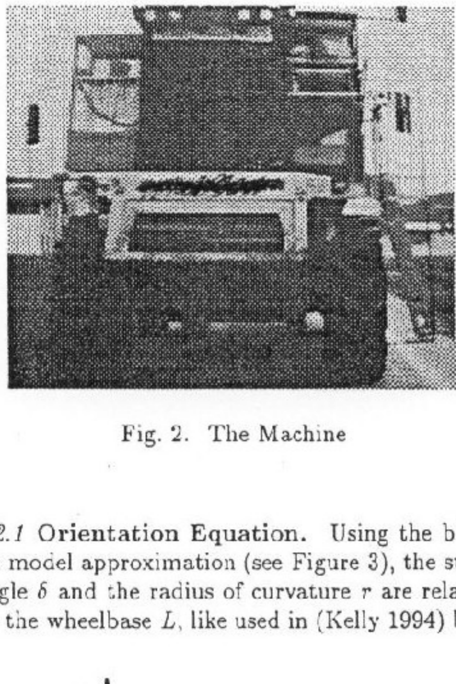

Fig. 2. The Machine

2.2.1 **Orientation Equation.** Using the bicycle model approximation (see Figure 3), the steer angle δ and the radius of curvature r are related by the wheelbase L, like used in (Kelly 1994) by:

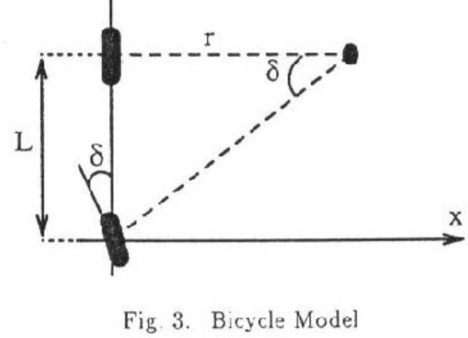

Fig. 3. Bicycle Model

$$\tan\delta = \frac{L}{r} \quad (18)$$

In Figure 4 we show a small portion of a circle ΔS representing the trajectory to realize by the machine. We assume that the machine moves with small displacements between an initial curvilinear abscissa S_0 and a final one named S_f such that:

$$\frac{1}{r} = \lim_{\Delta s \to 0} \frac{\Delta\psi}{\Delta S} = \frac{d\psi}{dS} \quad (19)$$

The dot of S englobes the longitudinal velocity along z axis and the lateral one along x axis. In fact, the rotation rate is obtained as:

$$\dot{\psi} = \frac{\tan\delta}{L}\sqrt{\dot{x}^2 + \dot{z}^2} \quad (20)$$

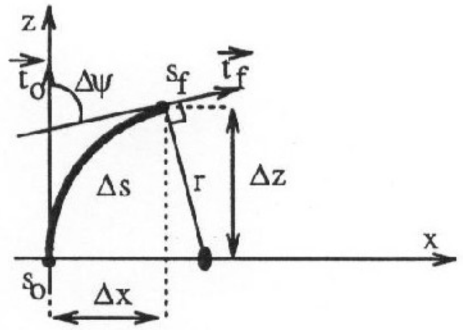

Fig. 4. Vehicle Trajectory with Linked Frame

2.2.2 **Lateral Position Equation.** The lateral position noted x can be computed by assuming that the machine moves with small displacements. In the case of a longitudinal motion along z axis during a lapse of time Δt, the machine moves with the distance Δz taking $\dot{z}$ as a longitudinal velocity (see Figure 4).
We express:

$$\Delta z = r\sin\Delta\psi \quad (21)$$

and

$$\Delta x = r(1 - \cos\Delta\psi) \quad (22)$$

By eliminating r from (21)and (22), we obtain:

$$\Delta x = \Delta z \frac{1 - \cos\Delta\psi}{\sin\Delta\psi} \quad (23)$$

Without loss of generality we can consider that the initial conditions are null since the frame is linked at the position s_0 and then $\Delta x = x$, $\Delta z = z$ and $\Delta\psi = \psi$. We compute the derivative over time of the lateral coordinate x of the machine given by (23) which depends on z and ψ, as follows:

$$\dot{x} = \frac{1 - \cos\psi}{\sin\psi}\left[\dot{z} + \frac{z\dot{\psi}}{\sin\psi}\right] \quad (24)$$

2.2.3 **Kinematic Model Equations.** The steering mechanism is modelled by equations (20) and (24) expressing the following coupled nonlinear differential equations:

$$\begin{cases} \frac{d\psi(t)}{dt} &= \frac{\tan\delta(t)}{L}\sqrt{\left[\frac{dx(t)}{dt}\right]^2 + \left[\frac{dz(t)}{dt}\right]^2} \\ \frac{dx(t)}{dt} &= \frac{1-\cos\psi(t)}{\sin\psi(t)}\left[\frac{dz(t)}{dt} + \frac{z(t)}{\sin\psi(t)}\frac{d\psi(t)}{dt}\right] \end{cases} \quad (2$$

The approximation to small angles (ψ and δ are less than 7^o) is valid in the case of our application and lets us to simplify equations of (25). This gives us the relation between the differential of the lateral coordinate x and the lateral deviation ψ with the steering angle δ by expressing the developpement of trigonometric equations to the second order. We can also consider that the machine moves with constant longitudinal speed $\dot{z} = V$ and that $\dot{x} << V$, we can write:

$$\dot{x} = \frac{\psi}{2}(\dot{z} + \frac{z}{\psi}\dot{\psi}) \quad (26)$$

Taking into account of the approximations below, we have $\dot{\psi} \approx \frac{\dot{z}}{r}$ and then $\psi = \frac{z}{r}$ since the r is constant and the initial conditions are null (frame fixed at initial position of the robot). We finally find the kinematic model of the machine expressed by the following equations which are similar to those obtained by an other method in (Khadraoui june-1995):

$$\begin{cases} \dot{\psi} &= \frac{V}{L}\delta \\ \dot{x} &= V\psi \end{cases} \quad (27)$$

3. CONTROLLER DESIGN

We treat here, single input linear system in the case of (θ, ρ) output parameters (see Figure 5). To control such a model, a technique of pole assignment is used. The Figure 5 represents different parts of the servoing chain such as:

- $\underline{s}^*$ is considered as a reference target image to be reached in the image frame,
- $\underline{s}$ is the value of visual information currently observed by the camera which is computed by image processing,
- G is the vector gain given by pole placement,
- $\underline{i}$ is the control variable of the machine representing the steering angle of the machine,

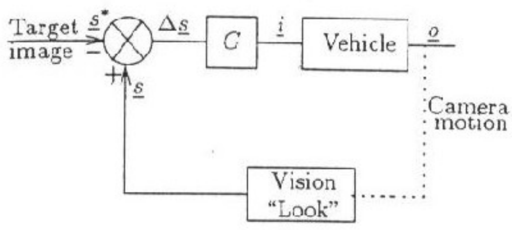

Fig. 5. Visual Servoing Approach

- $\underline{o}$ is the set of outputs characterizing the machine position and orientation.

3.1 Computation of the Interaction Matrix

First of all, we define the set of visual features to introduce in the control loop. In our case the parameters chosen as a state vector are:

$$\underline{s} = (\theta, \rho)^T \tag{28}$$

Then, the work consists of defining the interaction matrix related to the desired position $\underline{s} = \underline{s}^*$. This one represents the relation between the visual features and the velocity screw which defines the set of machine displacements. We have from (17):

$$\dot{\underline{s}} = L^T_{|\underline{s}=\underline{s}^*} \, T_c \tag{29}$$

The equation of the plane containing the desired

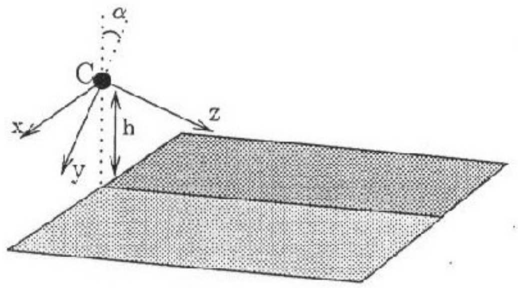

Fig. 6. Ground and Camera Reference

line and according to the camera reference is expressed as (see Figure 6):

$$\cos\alpha \, y - \sin\alpha \, z + h = 0 \tag{30}$$

Considering equation (17) and taking the desired features, such as $\theta = \theta^*$ and $\rho = \rho^*$, then the interaction matrix at the equilibrium situation is given by:

$$L^T_{|\underline{s}=\underline{s}^*} = \begin{pmatrix} \lambda^*_\theta \cos\theta^* & \lambda^*_\theta \sin\theta^* & -\lambda^*_\theta \rho^* & -\rho^* \cos\theta^* & -\rho^* \sin\theta^* & -1 \\ \lambda^*_\rho \cos\theta^* & \lambda^*_\rho \sin\theta^* & -\lambda^*_\rho \rho^* & (1+\rho^{*2})\sin\theta^* & -(1+\rho^{*2})\cos\theta^* & 0 \end{pmatrix} \tag{31}$$

with

$$\begin{cases} \lambda^*_\theta &= -(\cos\alpha \cos\theta^*)/h \\ \lambda^*_\rho &= (\cos\alpha \, \rho^* \sin\theta^* - \sin\alpha)/h \end{cases}$$

3.2 Continuous Control State Model

Here, we elaborate a state model which integrate both the model of the machine and the one of the scene. In the context of our application, we assimilate the machine to a particular mobile robot which moves with limited degrees of freedom. It has non-holonomic constraints since the number of degrees of freedom of control, δ in our case, is less than the number of degrees of freedom of displacement, translational motion according to x and z axis and rotational one around y axis. In our application, we are only interested in the lateral control of the machine. So, only the components of the interaction matrix related to the lateral velocity and the orientation one are kept. In fact, the interaction matrix is reduced to:

$$\dot{s} = \begin{bmatrix} l_{11} & l_{12} \\ l_{21} & l_{22} \end{bmatrix} \begin{pmatrix} V_x \\ \Omega_y \end{pmatrix} \tag{32}$$

with

$$\begin{cases} l_{11} &= \lambda^*_\theta \cos\theta^* \\ l_{12} &= \rho^* \sin\theta^* \\ l_{21} &= \lambda^*_\rho \cos\theta^* \\ l_{22} &= (1+\rho^{*2})\cos\theta^* \\ \lambda^*_\theta &= (\cos\alpha \cos\theta^*)/h \\ \lambda^*_\rho &= -(\cos\alpha \, \rho^* \sin\theta^* + \sin\alpha)/h \end{cases}$$

We remark that the velocities V_x and Ω_y correspond to those expressed in (27) for the machine. We write:

$$\begin{cases} V_x = \dot{x} &= V\psi \\ \Omega_y = \dot{\psi} &= \frac{V}{L}\delta \end{cases} \tag{33}$$

and

$$\begin{pmatrix} \dot{x} \\ \dot{\psi} \end{pmatrix} = \begin{bmatrix} l_{11} & l_{12} \\ l_{21} & l_{22} \end{bmatrix}^{-1} \begin{pmatrix} \dot{\theta} \\ \dot{\rho} \end{pmatrix} \tag{34}$$

By integrating (34) over time we have:

$$\begin{pmatrix} x \\ \psi \end{pmatrix} = \frac{1}{\Delta l} \begin{bmatrix} l_{22} & -l_{12} \\ -l_{21} & l_{11} \end{bmatrix} \begin{pmatrix} \theta \\ \rho \end{pmatrix} + \begin{bmatrix} k_1 \\ k_2 \end{bmatrix} \tag{35}$$

such as k_1 and k_2 are the constants of integration assuming that $l_{11} l_{22} \neq l_{21} l_{12}$. Using (33) and (35), we easily express the velocities V_x and Ω_y such as:

$$\begin{cases} V_x = \frac{V}{\Delta l}(-l_{21}\theta + l_{11}\rho) + k_2 V \\ \Omega_y = \frac{V}{L}\delta \end{cases} \tag{36}$$

with:

$$\Delta l = l_{11}l_{22} - l_{21}l_{12}$$

3.3 Pole Placement Design

After some developments, we lead to a linear 2-DOF model used for steering control system. The continuous-time state-space form of the model (32) becomes then:

$$\dot{\underline{s}} = A\,\underline{s} + B\,u + K\,I \tag{37}$$

where:

- $\underline{s}$ is the visual information vector to compute at each iteration by image processing.
- u is the control variable to inject to the system at each step of servoing task.
- A and B are constant matrices.
- K is a constant vector which depends on initial conditions.

with

$$s = \begin{pmatrix} \theta \\ \rho \end{pmatrix} \tag{38}$$

$$A = \frac{V}{\Delta l}\begin{bmatrix} -l_{11}l_{21} & l_{11}^2 \\ -l_{21}^2 & l_{11}l_{21} \end{bmatrix} \tag{39}$$

$$B = \frac{V}{L}\begin{bmatrix} l_{12} \\ l_{22} \end{bmatrix} \tag{40}$$

$$u = \delta \tag{41}$$

$$K = k_2 V \begin{bmatrix} l_{11} \\ l_{21} \end{bmatrix} \tag{42}$$

We introduce in the control loop the visual features θ and ρ of the line. The state representation of the system with initial conditions null ($k_2 = 0$) is given by:

$$\begin{pmatrix} \dot\theta \\ \dot\rho \end{pmatrix} = \frac{V}{\Delta l}\begin{bmatrix} -l_{11}l_{21} & l_{11}^2 \\ -l_{21}^2 & l_{11}l_{22} \end{bmatrix}\begin{pmatrix} \theta \\ \rho \end{pmatrix} +$$

$$\frac{V}{L}\begin{bmatrix} l_{12} \\ l_{21} \end{bmatrix}\delta \tag{43}$$

The control law is synthesized using a pole placement technique by assimilating the behaviour of the system to a second order system having ξ as a damping ratio and ω_0 as its frequency. It is expressed as follows:

$$u = G(\underline{s} - \underline{s}^*) \tag{44}$$

with:

$$G = \begin{pmatrix} g_1 & g_2 \end{pmatrix} \tag{45}$$

and then:

$$\begin{aligned} g_1 &= \frac{L\,\omega_0}{V^2\,\Delta l}(2\,V\,\xi\,l_{21} - \omega_0\,l_{22}) \\ g_2 &= -\frac{L\,\omega_0}{V^2\,\Delta l}(2\,V\,\xi\,l_{11} - \omega_0\,l_{12}) \end{aligned} \tag{46}$$

4. EXPERIMENTAL RESULTS

The simulations allow us to adjust different parameters that we use to compute the gains of the controller (parameters of the second order system ξ and ω_0, and the speed V of the machine). The experimental tests with the machine are realized with a white line drawn on the ground in order to optimize the image processing (see Figure 7). The

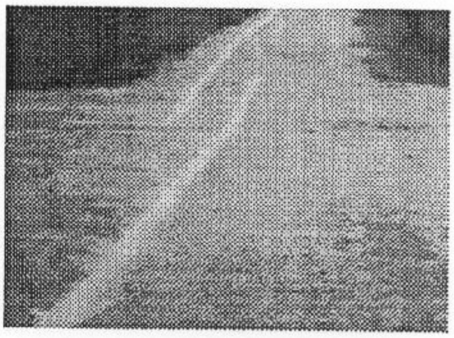

Fig. 7. Step Circuit

experimentation results confirm those obtained in simulations against that we do not take into account in simulation the real variation of the speed of the machine and the sampling period T_s due to algorithm of image processing. We tested our law in situations corresponding to those we can meet in a natural environment. The servoing task to accomplish consists of, at first to determine the response to a step of 1 meter distance between the two lines (see Figure 7), and at second to follow the line with good precision. In Figure 8 presented results are done with adapted parameters fixed in simulations in order to obtain good response of a second order system. We adjust the two parameters ξ and ω_0 with regard to the average speed of the machine which is fixed to $4km/h$. The result represented in Figure 8 concerns the lateral position x of the machine obtained both in simulation and in real experimentation, and the features errors used as the visual information. The experimental lateral position was reconstructed by putting an other camera perpendiculary to the scene taking into account of the camera calibration.

In Figure 9, we tested the robustness of the control law with regard to noise introduced in the measurement parameters ρ and θ. This noise represents really the variation of these parameters when the machine works in real conditions of mowing operations ($\approx 15\%$). At the last, we tested the robustness of the approach to the variation of the speed. The control is synthesized at a fixed velocity of $4km/h$ and the machine is gone at $10km/h$. Figure 10 shows that the machine reachs the line and continue following it against the variation of the speed V.

ω_0	ξ	$V(km/h)$	$T_s(ms)$
0.14	0.9	4	200

Speed: $4km/h$

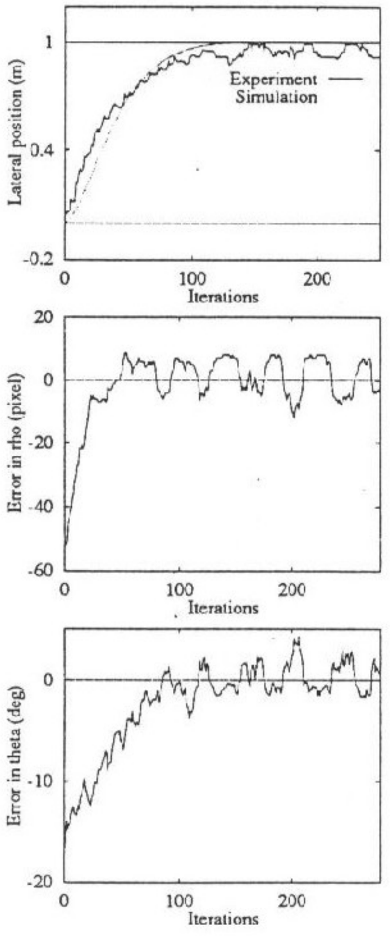

Fig. 8. Results with Adapted Parameters

The image processing algorithm, developped in (Derras 1993), use an original region segmentation based on a Markovian modelling of a set of sites. A control servoing unit calculates the trajectory which allows the mower to follow the limit by giving the value of (θ, ρ) at each iteration.

ω_0	ξ	$V(km/h)$	$T_s(ms)$
0.14	0.9	4	200

Speed: 4km/h

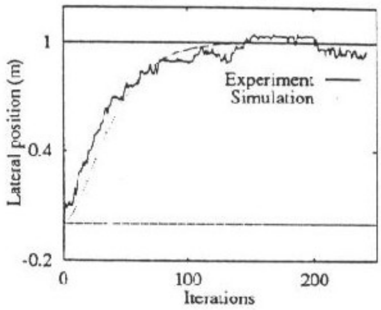

Fig. 9. Results with Noise Introduction

ω_0	ξ	$V(km/h)$	$T_s(ms)$
0.14	0.9	4	200

Speed: $10km/h$

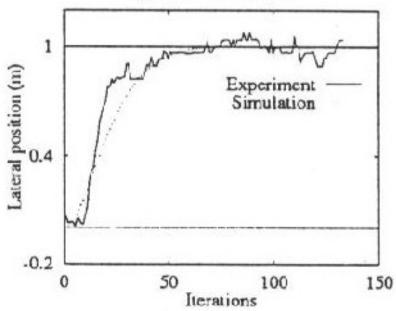

Fig. 10. Results with Speed Variation

5. CONCLUSION

In the approach presented here, the control is directly specified in terms of regulation in the image space. One can notice that this approach has the advantage of avoiding the intermediary step of 3D estimation of the environment with regard to the robot. This idea allows us to introduce in the control loop features measured in the same space. This prevents us from making bad estimation of 3D measures in the case of three dimensional control but we simply need to construct an interaction matrix related to the scene.

The gains of the control law developped are adaptive with regard to the desired situation to reach in the image space and to the machine speed. So, we do not need to a phase of empirical gains research like in (Debain october-1995) where it also used an other technique of visual servoing. One can remark that the machine is simply modelled by a kinematic equations and then we show that it is largely sufficient for this kind of applications. All the results obtained show a good convergency and robustness of our algorithm. They are good enough to demonstrate the feasibility of such an approach which can be extended for any other wheel mobile robot with steering direction.

REFERENCES

J. Amat, J.Battle, J.M. Fuertes, A.B. Martinez (1993) : *Vision Controlled Robot for agricultural Application*, 24th ISIR, pp.537-542, November 4-6, 1993.

F. Chaumette (1990) : *La relation vision-commande : théorie et application à des tâches robotiques*, Phd Thesis IRISA/INRIA, Rennes, France, July 1990.

C. Debain, M. Derras, M. Berducat, P. Bonton, J. Gallice (1994) : *Development of a Visual Guidance System for an Upkeep Robot of Natural Environments*, IMACS, SPRANN'94: International Symposium on Signal Processing, Robotics an Neural Networks, In cooperation with the IEEE/SMC society, pp.121-124, april 1994, Lille-France.

C. Debain, D. Khadraoui, M. Derras, P. Martinet, P. Bonton (1995) : *A Visual Servoing Approach to Control Agricultural Mobile Machines*, in International Advanced Robotics Programme, the fourth Workshop on Robotics in Agriculture and the Food-Industry, 30-31 october 1995, Toulouse-France.

M. Derras, M. Berducat, P. Bonton, J. Gallice, R. Canals (1993) : *Segmentation texturale originale appliquée au guidage visuel d'un robot d'entretien d'espaces naturels*, 14 ème colloque sur le traitement du signal et des images, GRETSI, Juan-les-pins, 13-16 septembre 1993, pp. 771-774.

B. Espiau, F. Chaumette, P. Rives (1992) : *A new Approach to Visual Servoing in Robotics*, in IEEE Trans. on Robotics and Automation, vol. 8, n.3, 1992.

R. Pissard-Gibollet, P. Rives (1991) : *Asservissement Visuel Appliqué à un Robot Mobile: état de l'art et modélisation cinématique*, Rapport de recherche No 1577, INRIA, Décembre 1991.

F. Jurie, P. Rives, J. Gallice and J.L.Brame (1994) : *High-speed vehicle guidance based on vision*, Control Eng. Practice, Vol.2, N0.2, pp.287-297.

R.A. Jarvis (1990) : *Omniescient Camera Based outdoor mobile robot*, in 1^{st} IARP Workshop on Robotics in Agriculture and the Food Industry, Avignon, France, 1990, pp. 247-258.

A. Kelly (1994) : *A partial Analysis of the High Speed Autonomous Navigation Problem*, Technical Report, The Robotics Institute Carnegie Mellon University, May 1994.

D. Khadraoui, G.Motyl, P. Martinet, J. Gallice, F. Chaumette (1995) : *Visual Servoing in Robotics Scheme Using a Camera/Laser-Stripe Sensor*, Publication interne IRISA n°898, Janvier 1995.

D. Khadraoui, P. Martinet, J. Gallice (1995) : *Linear Control of High Speed Vehicle in Image Space*, in the Second International Conference on Industrial Automation, June 1995, Nancy-France.

N.D. Klassen, R.J. Wilson, J.N. Wilson (1994) : *Guidance Systems for Agricultural Vehicles*, in EuroAgEng, International Commission of Agricultural Engineering. The 12^{th} World Congress on Agricultural Engineering, Milano, August 29-September 1^{st}, pp. 1136-1142.

G. Motyl, P.Martinet, J.Gallice (1993) : *Visual servoing with respect to a target Sphere Using a Camera/laser-stripe sensor*, in proceedings: '93 International Conference on Advanced Robotics, Tokyo, Japan, pp. 591-596 November 1-2, 1993.

G. Sandini, F. Buemi, M. Massa, M. Zucchini (1990) : *Visually guided operations in green houses*, in 1^{st} IARP Workshop on Robotics in Agriculture and the Food Industry, Avignon, France, 1990, pp. 69-84.